Assembly, electrochemical characterisation and electrocatalytic ability of multilayer films based on $[Fe(bpy)_3]^{2+}$, and the Dawson heteropolyanion, $[P_2W_{18}O_{62}]^{6-}$.

Nigel Fay, Eithne Dempsey and Timothy McCormac*

Electrochemical Technology Research Centre

Department of Applied Science

Institute of Technology Tallaght

Dublin 24

Ireland

Abstract

Successive adsorption onto a glassy carbon electrode of the Dawson heteropolyanion, $[P_2W_{18}O_{62}]^{6-}$, and the multiply charged cation $[Fe(bpy)_3]^{2+}$, resulted in the formation of stable multilayer assemblies on the electrode surface. Surface coverages were found to be typical of monolayer coverages for multilayer systems. Cyclic voltammetric studies of the assembly in aqueous. 0.5M $NaHSO_4$, gave a range of redox couples associated with the $Fe^{3+/2+}$ redox system, of the cationic $[Fe(bpy)_3]^{2+}$ moiety and the tungsten-oxo framework of the Dawson parent heteropolyanion, $[P_2W_{18}O_{62}]^{6-}$. It was possible to immobilise up to thirty monolayers, with the system exhibiting well behaved redox behaviour. The stability of the assembly towards redox switching was investigated, with it being found be extremely stable once the outer layer is anionic in nature. The

immobilised film was also tested for electrocatalytic activity for the reduction of nitrite, hydrogen peroxide and bromate, and was shown to be an efficient electrocatalyst.

Keywords: *Dawson heteropolyanion,* *$[Fe(bpy)_3]^{2+}$,* *multilayer assemblies, electroctrocatalysis..*

**to whom correspondence should be addressed*

Email: tim.mccormac@it-tallaght.ie

Fax: +353-1-4074200 Tel: +353-1-4042814

1. Introduction

Over the past several years, there has been a great deal of interest in the self-assembly of ordered molecular arrays formed spontaneously as monolayers on solid surfaces upon immersion in a solution of the respective adsorbate molecules [1]. The technique of consecutive adsorption of anionic and cationic layers has been well documented by, for example, Decher *et al.* [2-4] who reported on various systems involving these electrostatic interactions. Films with alternating layers of the anion cobalt phthalocyanine tetrasulphonate and cationic polydimethyldiallylammonium chloride prepared by electrostatic layer-by-layer adsorption were reported by Lvov *et al.* [5]. Heteropolyanions (HPAs) are still a rapidly growing class of compounds with various applications ranging from catalysis to analytical chemistry and medicine [6,7], their use as the anionic moiety in self-assembled multilayers has been studied extensively. Previously, researchers [8, 9] exploited the ability of HPAs to attract and bond multiply-charged cations to construct multiple layers of HPA salts on electrode surfaces. A monolayer of HPA ($P_2Mo_{18}O_{62}^{6-}$, $P_2W_{17}CrO_{61}^{7-}$, $P_2W_{17}FeO_{61}^{7-}$, $PW_{11}CrO_{39}^{4-}$) was adsorbed from solution onto the electrode surface, followed by cations such as NH_3^+, $(CH_2)_XNH_3^+$, Hg_2^{2+} and Ag^+. The redox characteristics of these multilayer systems, along with their stability, were also reported. Kulesza *et al.* [10] described the use of Keggin HPAs as inorganic templates for monolayers and multilayers of ultrathin polyaniline. EQCM was used to study the assemblies when adsorbed on electrode surfaces. Wang *et al.* [11] recently reported on the self-assembly of multilayer films based on a Keggin-type polyoxometalate, namely $SiW_{12}O_{40}^{4-}$, and polyaniline.

These types of multilayer assemblies incorporating HPAs have also been tested for their electrocatalytic properties **towards analytes such as ascorbic acid [12], nitrite [13], bromate and hydrogen peroxide [14, 15].** Recently, Kuhn *et al.* [16] described a procedure for the deposition of multilayers of $Os(bpy)_3^{2+}$-$P_2Mo_{18}O_{62}^{6-}$ on various electrode surfaces, including glassy carbon, highly ordered pyrolytic carbon, indium tin oxide and gold-coated quartz. Multilayer films which were stable up to twenty layers were formed. This procedure was also quite rapid and eliminated the need to dry the coating between each immersion step. The electrochemistry of the assembly is studied. The same group followed on from this work when reporting on the electrochemical reduction of NO_2^- and the oxidation of benzyl alcohol using multilayers consisting of $P_2Mo_{18}O_{62}^{6-}$ anions and $Os(bpy)_3^{2+}$ or $Ru(bpy)_3^{2+}$ cations [17]. It was found that all but the first anionic layer in the multilayer coatings contribute little to the catalytic activity of the coatings.

In our paper we report on the formation of extremely stable multilayer films based upon the parent Dawson type HPA, $[P_2W_{18}O_{62}]^{6-}$, and $[Fe(bpy)_3]^{2+}$. It was found that up to and beyond thirty stable monolayers could be deposited onto a glassy carbon electrode. This coverage exceeds those of previously studied multilayer systems such as those of Kuhn and Anson [16]. Also our system exhibits clear electrochemical redox activity for both the HPA and the $[Fe(bpy)_3]^{2+}$ moieties, again this is in contrast with previous work from Kuhn and Anson on their system [16]. Finally we report on the electrocatalytic ability towards the reduction of various analytes, such as nitrite, bromate and hydrogen peroxide.

2. Experimental

2.1. Materials

$K_6P_2W_{18}O_{62}$ and $[Fe(bpy)_3]Cl_2$ were synthesised and characterised according to the literature [18,19].All chemicals were of reagent grade, purchased from Aldrich and used as received. Deionised water was utilised when preparing electrolytes and buffers, while HPLC grade water was used in the formation of multilayer assemblies. Aqueous buffer solutions were prepared from the following solutions, which were either adjusted with 0.1M NaOH or 0.1M H_2SO_4; 0.1M Na_2SO_4 (pH 2 to 3), 0.1M Na_2SO_4 + 20mM CH_3COOH (pH 3.5 to 5.0) and 0.1M Na_2SO_4 + 20mM NaH_2PO_4 (pH 5.5 to 7.0).

2.2. Apparatus and Procedures

A CHI 660A potentiostat was employed for all electrochemical experiments. Electrochemical experiments were performed in a single compartment three-electrode cell. A silver/silver chloride (3 M KCl) reference electrode was used for the aqueous electrochemistry. A vitreous carbon (d=3mm) electrode was employed as the working electrode. The auxiliary electrode material was a platinum wire. The working electrode were polished successively with 1.0, 0.3 and 0.05µm aqueous alumina slurries and sonicated in distilled water and rinsed with acetone after each polishing step. All solutions were degassed with pure argon for 15 min prior to electrochemical experiments.

Multilayer Assembly

Alternating ionic multilayer films were attached using the following procedure. A glassy carbon electrode was firstly roughened by polishing with 0.3µm alumina. This electrode

was immersed in a 0.5mM solution of $P_2W_{18}O_{62}^{6-}$ in 0.5M $NaHSO_4$ (pH=1.1) for 20 min, to allow an initial HPA monolayer to adsorb. The electrode was then soaked in HPLC grade water for five minutes. The coated electrode was next transferred to a 0.5M $NaHSO_4$ supporting electrolyte solution and a cyclic voltammogram recorded. This was followed by immersion of the electrode in an aqueous electrolyte free 0.5mM $Fe(bpy)_3^{2+}$ solution for 10 min. After another soaking of this electrode in HPLC grade water, it was soaked in a 0.5mM electrolyte free solution of $P_2W_{18}O_{62}^{6-}$ in water. This procedure was repeated in order to build up a series of ionic layers. By soaking the modified electrode in HPLC grade water between layers, this prevented anions/cations from the electrolyte being adsorbed.

3. Results and Discussion

3.1. Electrochemical Characterisation of Assembled Multilayers of $Fe(bpy)_3^{2+}$-$P_2W_{18}O_{62}^{6-}$ with outer anionic layer

The electrochemical activity of the $P_2W_{18}O_{62}^{6-}$ anion in solution consists of a series of mono- and bielectronic redox waves associated with the redox activity of the tungsten-oxo framework. Figure 1(a) illustrates the behaviour of the parent HPA in 0.5M $NaHSO_4$. The first two redox couples, with $E_{1/2}$ values of -0.061 and -0.243V, are pH independent and monoelectronic in character, with the last two, $E_{1/2}$ values of -0.527 and -0.771V, being pH dependent bielectronic waves. Therefore in this medium the parent HPA can accept up to 6 electrons reversibly without structural modification.

Figure 1(b) shows a cyclic voltammogram of a multilayer film of $Fe(bpy)_3^{2+}$-$P_2W_{18}O_{62}^{6-}$ in aq. 0.5M $NaHSO_4$, when the potential window is extended to +1.25V and the outer layer is anionic. It is clear that electrochemical responses associated with both moieties within the multilayer system are accessible, and well defined, for both the tungsten-oxo framework of the anionic HPA moiety, with $E_{1/2}$'s of -0.215, -0.404, and -0.637 V. These correspond to the following redox switching states of the HPA, $P_2W_{18}O_{62}^{6-/8-}$, $P_2W_{18}O_{62}^{8-/10-}$ and $P_2W_{18}O_{62}^{10-/12-}$, respectively, this is ignoring the addition of two protons, H^+, for each of the redox couples. Also what is apparent is the presence of the $Fe^{2+/3+}$ redox process associated with the cationic $Fe(bpy)_3^{2+}$, with an $E_{1/2}$ of +0.853 V. The former redox processes all exhibit peak to peak (ΔE_p) separations of less than 20mV, typical for a surface confined species illustrating fast redox switching dynamics. However, interestingly the $Fe^{2+/3+}$ redox process possesses an ΔE_p of 86 mV, hence not typical of

surface confined behaviour. The reason for this is probably due to the fact that upon redox switching of the Fe^{2+} metal centre a charge compensating anion from the background electrolyte must pass into the multilayer system for reasons of charge neutrality. Due to the outer layer being anionic in character, namely the HPA, then some charge repulsion more than likely occurs between the charge compensating anion and outer anionic charge situated on the HPA. Importantly our system possesses a clear advantage over some other similar systems that have been reported, in that it is possible to electrochemically switch the underlying cationic layer between its redox states. For example, Kuhn and Anson [16] were not able to get a clear electrochemical response for $Os^{2+/3+}$ in their system, when the outer layer was anionic.

For the case of non-interacting neighbours within a film the full width at half-maximum (FWHM) for a surface wave should be 90.6/*n* mV where *n* is the number of electrons involved [bard Faulkner]. For the first, second and third waves in Figure 1(b) the values for FWHM are 94, 6**8** and **75**mV respectively. These values are higher than the anticipated 45.3mV expected for a two-electron process. This can be explained by the fact that it is well known that FWHM values higher than what is expected reflect repulsive interactions within the film [20, 21].

A scan rate study was performed on a $Fe(bpy)_3^{2+}$-$P_2W_{18}O_{62}^{6-}$ deposited multilayer which contained thirteen monolayers of coverage. Figure 1(c) displays the voltammetric tungsten-oxo responses for the modified electrode in aq. 0.5M $NaHSO_4$ solution, pH = 1.1, as a function of scan rate. It was found that the peak potentials associated with the

tungsten-oxo framework were independent of scan rate and that the peak currents were directly proportional to scan rates of up to $1Vs^{-1}$ this being indicative of surface controlled processes. At scan rates beyond 1 Vs^{-1}, the film exhibits diffusion controlled redox processes as is illustrated graphically in figure 1(d).

Figure 2(a) is a cyclic voltammogram showing the deposition from one to 23 alternating ionic layers on a GCE, when the outer layer is anionic. The electrochemical behaviour of these couples remained the same during the deposition of up to 30 monolayers. Following deposition of each layer of $P_2W_{18}O_{62}^{6-}$ the tungsten-oxo peak currents increase in a step-wise fashion corresponding to the addition of a single monolayer. This means all the adsorbed molecules are in contact with the surface layer of the adsorbent. Figure 2(b) illustrates that the surface coverage (Γ), on a glassy carbon electrode, is directly proportional to the number of layers of $Fe(bpy)_3^{2+}$ and $P_2W_{18}O_{62}^{6-}$ adsorbed. From this data the average surface coverage associated with one monolayer was found to be 1.39 x 10^{-11} mol cm^{-2}, this value being typical of monolayer coverages for multilayer systems [**20**]. Also, the fact that the cationic moiety is present in the multilayer film is clear, as if the coating is not exposed to a solution of $Fe(bpy)_3^{2+}$ no increase in the surface coverages or the peak currents for the tungsten-oxo processes are observed.

The acidity of the supporting electrolyte was also shown to have a marked effect upon the electrochemical behaviour of the multilayer system. It is well known [18] that the $P_2W_{18}O_{62}^{6-}$ species is stable in pH's from 2.00 to 8.00. With increasing pH, the three tungsten redox peaks move to more negative potentials with the two bielectronic couples

showing a shift of 60-75 mV per pH unit, corresponding to approximately the addition of two protons, as observed with the solution phase species [15], while only one proton is added for the first monoelectronic couple resulting in a shift of 35-40mV per pH unit. These results are summarised in Table 1.

Table 2 contains the stability data for the multilayer system at the two separate pH values namely 1.10 and 4.00, for each of the tungsten-oxo based redox processes. What is evident from the data is that the film exhibits greater stability at more acidic pH values. We believe this to be linked to the pH dependent nature of the tungsten-oxo reductions, when at more alkaline pH's the availability of protons which accompany the reductions is less, relative to that in pH 1.10. Therefore the redox processes for the tungsten-oxo redox processes at pH 4.00 are rendered less stable.

Among the factors that affect the adsorption of the $P_2W_{18}O_{62}^{6-}$ is the pH of the solution from which the adsorption occurs. In previous multilayer systems, based on isopolyanions, it is known that the presence of protons in the adsorption solution significantly enhances the quantity of the anion that is reversibly adsorbed [16]. In addition to this when 0.5M Na_2SO_4 is used as the electrolyte instead of 0.5M $NaHSO_4$ there is a lower amount of the anion adsorbed, proving it is indeed the presence of protons and not the ionic strength that causes this strong absorption between the anion and the electrode. It was found that the peak currents associated with the tungsten-oxo framework were in the range of 1.4×10^{-6} to 2.0×10^{-6} A when the solution from which the anion is adsorbed is aqueous 0.5M $NaHSO_4$, and only 2.5×10^{-7} to 7.0×10^{-7} A with

poorer ill defined redox processes, when the solution is the more alkaline aqueous 0.5M Na_2SO_4.

3.2. Electrochemical Characterisation of Assembled Multilayers of $Fe(bpy)_3^{2+}$-$P_2W_{18}O_{62}^{6-}$ with outer cationic layer

Up to this point the multilayers that have been discussed are those that are comprised of an outer HPA anionic layer. Figure 3(a) is a cyclic voltammogram showing the step by step assembly of up to twenty alternating ionic layers on a GCE, when the outer layer is the cationic $Fe(bpy)_3^{2+}$. The potential of the $Fe^{2+/3+}$ couple, $E_{1/2}$ of +0.828 V, is close to that exhibited by the same cation in solution, $E_{1/2}$ of +0.820 V. Following deposition of each layer of $Fe(bpy)_3^{2+}$, the peak currents increase in a step-wise fashion corresponding to the addition of one monolayer, namely 1.39 x 10^{-11} mol cm^{-2}, which is typical of monolayer coverages for multilayer systems [20]. Also, the fact that the anionic moiety is present in the multilayer film is clear, as if the coating is not exposed to a solution of $P_2W_{18}O_{62}^{6-}$ no increase in the surface coverages or the peak currents for the $Fe^{2+/3+}$ processes are observed.

As with the previous multilayer system in section 3.1, a stability study was performed and the results are shown in Figure 3(b). Twenty monolayers were deposited on a GCE, and the modified electrode was then cycled in aq. 0.5M $NaHSO_4$ electrolyte. Shown are CV segments after 1, 101, 201, 301, 401, 501, 601 and 701 cycles, and it is clear that there is a huge decrease in percentage global electroactivity upon cycling, as after 400 cycles the $Fe^{2+/3+}$ redox process has nearly disappeared, and i_{pa} has decreased from

1.830 x 10^{-6} A to 8.571 x 10^{-7} A. This indicates the film is much more stable when the outer layer is anionic. This may be due to the fact that the initial monolayer of anion is involved in adsorption to the glassy carbon electrode, and is followed by a series of electrostatic bilayers when the outer layer is anionic. However, when the outermost layer is cationic the assembled multilayer is destabilised significantly.

The intense absorbance of the tungsten-xo framework of the HPA provided a useful independent means of determining the presence of the HPA in the multilayer system. The multilayer film yielded two maxima in the spectra, at 244.6 and 307.2 nm. Both absorbances are attributed to the tungsten-oxo framework of the $P_2W_{18}O_{62}^{6-}$, as seen in UV/Vis spectra of α/β-$K_6P_2W_{18}O_{62}.15H_2O$ [18]. Figures 4(a) and 4(b) show the linear relationship between the number of adsorbed bilayers and the absorbance for the waves at 244.6 and 307.2 nm respectively. This near linear enhancement indicates a progressive assembly with an almost equal number of deposited heteeropolyanions in each cycle, which shows the highly reproducible nature of the layer-by-layer technique for multilayer assembly.

3.3 Cyclic voltammetry of Multilayer System in the Presence of Solution Redox Species

A thorough understanding of solute transport through thin films is important in describing the catalytic or inhibitory behaviour of such films [21]. Solute permeation is relevant to processes in ultathin films, and membranes such as drug encapsulation polymers [22], zeolite particles [23] and surfactant micellar structures [24]. Electrodes coated with

multilayer films were examined by cyclic voltammetry in the presence of potassium ferricyanide, $K_3Fe(CN)_6$, which undergoes a one-electron reduction at less negative potentials ($E_{1/2}$ = +0.400V vs Ag/AgCl) than those associated with tungsten-oxo cage of the heteropolyanion within the multilayer system. A representative cyclic voltammogram of ferricyanide at a bare GCE is shown in figure 5(a). In principle, ferricyanide may be reduced at the electrode/multilayer interface, after diffusion through the continuous multilayer system, or at the multilayer/solution interface by electron-transfer mediation by redox sites in the multilayer film.

Nine alternating layers of $P_2W_{18}O_{62}^{6-}$ and $Fe(bpy)_3^{2+}$ were then deposited on a GCE, and a CV of the film was carried out in 0.5M $NaHSO_4$, this is illustrated in figure 5(b). The film was stabilised in 0.5M $NaHSO_4$ was then transferred to a fresh 0.5M $NaHSO_4$ solution which contained 1mM potassium ferricyanide. The resulting cyclic voltammogram is shown in figure 5(c). What is immediately apparent on comparison between figures 5(a) and (c) is that the peak-to-peak separation for the ferricyanide has substantially increased from 60mV to 522mV in the presence of the multilayers on the electrode surface. However the currents associated with the reduction and reoxidation of the Fe^{3+} centre have remained virtually unchanged. These results indicate that the ferricyanide is able to penetrate the multilayer system and react at the underlying bare electrode but that there is a strong repulsion between the outer anionic heteropolyanion layer and the ferricyanide thus contributing to the large increase in the peak to peak separations. The presence of the ferricyanide has also had an effect upon the current associated with the first redox process of the HPA within the multilayer. There is an

increase in the associated reduction current and a corresponding decrease in the oxidative current for the $[P_2W_{18}O_{62}]^{6-/7-}$ couple. This implies that the reduced form of the HPA is mediating the reduction of the ferricyanide to ferrocyanide, with the $[P_2W_{18}O_{62}]^{7-}$ being chemically reoxidised to the $[P_2W_{18}O_{62}]^{6-}$ redox form. This reaction would account for the drastic reduction in the current associated with the reoxidation of the $[P_2W_{18}O_{62}]^{7-}$.

The effect of the film thickness upon the penetration of the ferricyanide through the film was investigated. Two films with thicknesses of 11 and 17 layers were utilised, with both systems it was found that ferricyanide could still penetrate through and react at the underlying electrode surface. Therefore we can conclude that the multilayer films must be quite porous.

3.3. Demonstration of electrocatalytic ability of multilayer assemblies of $Fe(bpy)_3^{2+}$-$P_2W_{18}O_{62}^{6-}$

3.3.1. Nitrite Reduction

Nitrite is a common pollutant from both agricultural and industrial sources.

Porphyrins have been used extensively for the electrochemical reduction of nitrite [26-29] but an unwanted side product of hydroxylamine is formed. Redox polymer films have also been utilised in nitrite reduction [30], but the polymer film formed was found to swell when immersed in electrolyte solution. Many heteropolyanion systems [31-36] have been employed for the electrocatalytic reduction of nitrite in the past. When investigating the electrocatalytic reduction of nitrite it is important to keep the pH of the solution above 4.0, to ensure NO_2^- is the species in the majority, due to

disproportionation reaction of the acidic form of nitrite at pH values more acidic than 3.5. Therefore the electrocatalytic experiments were performed at pH 4.5. A multilayer film $Fe(bpy)_3^{2+}$- $P_2W_{18}O_{62}^{6-}$ was adsorbed onto a glassy carbon electrode. The modified electrode was then tested to see if it maintained the electrocatalytic capabilities of the HPA in solution for nitrite reduction.

Figure 5(a) shows the overlap cyclic voltammograms of the multilayer assembly in buffer pH 4.5 (inner curve) and the resulting voltammogram obtained upon the addition of 0.4mM NO_2^- (outer curve). What is immediately apparent is the effect upon the last redox process of the HPA, with an increase in the associated reduction current and a subsequent decrease in the oxidation current. This enhanced current cannot be due to the reaction of NO_2^- at the underlying bare electrode as it has previously been shown [34] that the nitrite at this concentration, pH and potential, does not react at a bare carbon electrode.

The conclusion is that there is a catalytic reaction between multiply reduced HPA within the assembly and the NO_2^-. Upon successive additions of $NaNO_2$ there is an increase in this catalytic current. as seen by the increase in peak current of the first tungsten couple upon reduction. Interestingly previous published work [34] has shown that for the parent HPA in a buffered pH 4.60 solution, up to 30mM $NaNO_2$ needs to be added in order to get an electrocatalyic response. Therefore our system shows better electrocatalytic activity at low NO_2^- concentrations at pH 4.50, and does not require as high an overpotential. The fact that $Fe(bpy)_3^{2+}$- $P_2W_{18}O_{62}^{6-}$ is strongly attached to the electrode

surface is also a real advantage, but there are still two problems with this system as an effective electrocatalyst for nitrite reduction.

The multilayer system was also tested for the electrocatalytic reduction of nitrite when the outer layer was cationic. All conditions were identical to those utilised previously, and it was shown that the catalytic current observed was considerably less when the $[Fe(bpy)_3]^{2+}$ was the outer layer. For example upon the addition of 5mM NO_2^- the catalytic current is over 2μA, when the outer layer is anionic, whilst it is less than 1μA when the outer layer is the cationic $[Fe(bpy)_3]^{2+}$. This is likely to be due to the decreased stability of the multilayer system when the outer layer is cationic, as described previously.

3.3.2. Bromate Reduction

Bromate is a disinfectant by-product contaminant found in drinking water, and is formed during the ozonation of source water containing bromide. The overpotential for BrO_3^- reduction is high and therefore an efficient electrocatalyst would be beneficial. Various types of systems have been reported for bromate detection in the recent past [37, 38]. In addition several HPA systems have been employed for the reduction of bromate [14, 15, 38]. In this contribution thirteen layers of alternating $[P_2W_{18}O_{62}]^{6-}$ and $[Fe(bpy)_3]^{2+}$ were attached to a glassy carbon electrode surface as described earlier. Cyclic voltammetry was performed on this electrode in aq. 0.5M $NaHSO_4$. Figure 15(b) displays a series of voltammetric responses upon addition from 0.1 to 1 mM $NaBrO_3$. The increase in the reductive currents of the tungsten-oxo processes is pronounced, even at such a low

concentration of BrO_3^-. The increase in current however is in the last, most negative, tungsten-oxo process. This indicates it is the multiply reduced Dawson HPA that interacts with the BrO_3^-, to cause its reduction. Figure 16 displays a graph of BrO_3^- concentration versus catalytic current, and highlights the linear correlation between the two.

3.3.3. Hydrogen Peroxide Reduction

A range of heteropolyanions [40–43] have been investigated over the past number of years for into their ability towards the electrocatalytic reduction of hydrogen peroxide, H_2O_2. To investigate whether or not our system would act as an efficient electrocatalyst for H_2O_2 reduction, thirteen alternating ionic layers of $P_2W_{18}O_{62}^{6-}$ and $Fe(bpy)_3^{2+}$ were adsorbed onto a freshly polished GCE and the modified electrode cycled in aq. pH 4.6 buffer. Aliquots of H_2O_2 were added to the electrolyte, and voltammetric responses are shown in Figure 17(b) for concentrations from 0.1 to 0.3mM H_2O_2. The first point to observe is that when the potential is extended to the most negative tungsten the response tails off, and thus the low potential is set at -0.75 V. The increase in current is from the first tungsten couple, with an $E_{1/2}$ of -0.407 V, and therefore it is the first reduced form of the HPA which is catalysing the reduction of H_2O_2. The electrochemical response for the first tungsten-oxo process is difficult to see at pH 4.5, and therefore upon successive additions of H_2O_2 it appears that a 'new' wave is being formed. The clear response of this tungsten-oxo process was used to show the increase in catalytic current in relation to the concentration of H_2O_2, as shown in Figure 18.

The results obtained from these multilayer assemblies show that the electrode coating had catalytic activity for nitrite, NO_2^-, hydrogen peroxide, H_2O_2 and bromate, BrO_3^-.

However, coatings with multiple layers of catalyst did not exhibit activities that were much greater than those that contained only a single layer of catalyst. This is in good agreement with the $[Os(bpy)_3]_3.[P_2W_{18}O_{62}]$ system reported by Kloster and Anson [17], and is believed to be due to the fact that the first adsorbed layer contains most of the anions that contribute to the voltammetric responses and, presumably, to the catalysis of electrode reactions. This is the reason that the catalytic currents did not increase proportional to the coating thickness.

4. Conclusion

- Multilayer assemblies of $Fe(bpy)_3^{2+}$-$P_2W_{18}O_{62}$, containing over 30 layers, have been formed using electrostatic attractions, and have been shown to be both stable and reproducible. These multilayers were shown to exhibit the same pH dependence of the tungsten-oxo framework of the HPA in solution, and also were seen to maintain the same scan rate characteristics of thin films of these types of compounds.
- The multilayer film of $Fe(bpy)_3^{2+}$-$P_2W_{18}O_{62}$ was proven to be permeable, allowing the passage of bulky ions through the material to the electrode surface. The solute ions exhibited electrochemical responses at the modified electrode, with membrane diffusion and electron-transfer mediation being the likely modes of reaction.
- Unlike other multilayer systems of this type, a clear redox couple is observed for the cationic $Fe^{2+/3+}$ process, when the outer layer of the multilayer array is anionic.
- The $Fe(bpy)_3^{2+}$-$P_2W_{18}O_{62}$ assembly exhibited electrocatalytic responses for NO_2^-, H_2O_2 and BrO_3^-. However, the catalytic responses were not proportional to the

number of layers present, and it is therefore likely that the initial adsorbed layer of HPA contributes the catalytic responses of the electrode reactions.

5. Bibliography

[1] Ulman, A. An Introduction to Ultrathin Organic films. Academic Press, New York, 1991.

[2] Decher, G.; Hong, J.D. Makromol.Chem.,Macromol.Syrp. 1991, 46, 321.

[3] Decher, G.; Lvov, Y.; Schmitt, J. Thin.Film.Solids. 1994, 244, 772.

[4] Lvov, Y.; Decher, G.; Mohwald, H. Langmuir. 1993, 9, 481.

[5] Lvov, Y.; Kamau, G.N.; Zhou, D.L.; Rusling, J.F. J.Colloid and Interface Sci. 1999, 212, 570.

[6] M. T. Pope, Heteropoly and Isopoly Oxometallates, Springer, Berlin, 1983.

[7] J. E. Toth, F. C. Anson, J. Electroanal. Chem., 256, 1998, 361.

[8] Ingersoll, D.; Kulesza, P.J.; Faulkner, L.R. J.Electrochem.Soc. 1994, 141, 140.

[9] Kuhn, A.; Mano, N.; Vidal, C. J.Electroanal.Chem. 1999, 462, 187.

[10] Kulesza, P.J.; Chojak, M.; Miecznikowski, K.; Lewera, A.; Malik, M.A.; Kuhn, A. Electrochem.Commun.4. 2002, 4, 510.

[11] Wang, Y.; Guo, C.; Chen, Y.; Hu, C.; Yu, W. J.Colloid and Interface Sci. 2003, 264, 176.

[12] Sun, C.; Zhang, J. Electrochim.Acta. 1998, 43, 943.

[13] Li, L.; Sun, C. Mat.Chem.and Phys. 2001, 69, 45.

[14] Cheng, L.; Liu, J.; Dong, S. Anal.Chim.Acta. 2000, 417, 133.

[15] Zhai, S.; Gong, S.; Jiang, J.; Dong, S.; Li, J. Anal.Chim.Acta. 2003, 486, 85.

[16] Kuhn, A.; Anson, F.C. Langmuir. 1996, 12, 5481.

[17] Kloster, G.M.; Anson, F.C Electrochim. Acta. 1999, 44, 2271.

[18] McCormac, T.; Fabre, B.; Bidan, G. J.Electroanal.Chem. 1997, 425, 49.

[19] Basolo, F.; Dwyer, F.P. J. Am. Chem. Soc., 1954, 76, 1454.

[20] Bard, A.J.; Faulkner, L.R. Electrochemical Methods. Wiley & Sons Inc. New York. 2001.

[21] Ikeda, T.; Schmehl, R.; Danisevich, P.; Willman, K.; Murray, R.W. J. Am. Chem. Soc. 1982, 104, 10.

[22] Kydonieus, A.F. Controlled Release Technologies, C.R.C. Press, Cleveland, Ohio, 1980, Vol. 1.

[23] Eberly, P.E. Zeolite Chemistry and Catalysis. ACS Press, New York, 1976.

[24] Fendler, J.H.; Fendler, E.J. Catalysis in Micellar and Macromolecular Systems. Academic Press, New York, 1975.

[25] Peerce, P.J.; Bard, A.J. J.Electroanal.Chem. 1980, 112, 97.

[26] Cheng, S.H.; Su, Y.O. Inorg.Chem. 1994, 33, 5847.

[27] Yu, C.H.; Su, Y.O. J.Electroanal.Chem. 1994, 368, 323.

[28] Bradley, M.H.; Rhodes, M.R.; Meyer, T.J. Inorg.Chem. 1987, 26, 1746.

[29] Younathan, J.N.; Wood, K.S.; Meyer, T.J. Inorg.Chem. 1992, 31, 3280.

[30] Doherty, A.P.; Vos, J.G. J.Chem.Soc., Faraday Trans. 1992, 88, 2903.

[31] Dong, S.; Xi, X.; Tian, M. J.Electroanal.Chem. 1995, 385, 227.

[32] Keita, B.; Belhouari, A.; Nadjo, L.; Contant, R. J.Electroanal.Chem. 1995, 381, 243.

[33] Xi, X.; Dong, S. J.Mol.Catal.A: Chemical 1996, 114, 257.

[34] McCormac, T.; Bidan, B.; Fabre, G. J.Electroanal.Chem. 1997, 427, 155.

[35] Keita, B.; Girard, F.; Nadjo, L.; Contant, R.; Abbessi, M. J.Electroanal.Chem. 2001, 508, 70.

[36] Song, W.B.; Wang, X.H.; Liu, Y.; Liu, J.F.; Xu, H.D. J.Electroanal.Chem. 1999, 476, 85.

[37] Esteves da Silva, J.; Dias, J.; Magalhaes, J. Anal.Chim.Acta. 2001, 450, 175.

[38] Wagner, H.P.; Pepich, B.V.; Hautman, D.; Munch, D.J. J.of Chromatography. 2002, 956, 93.

[39] Rong, C.; Anson, F.C. Inorg.Chim.Acta. 1996, 242, 11.

[40] Dong, S.; Liu, M. J.Electroanal.Chem. 1994, 372, 95.

[41] Toth, J.E.; Melton, J.D.; Cabelli, D.; Bielski, B.H.J.; Anson, F.C. Inorg.Chem. 1990, 29, 1952.

[42] Bart, J.C.; Anson, F.C. J.Electroanal.Chem. 1995, 390, 11.

[43] Kuznetsova, N.I.; Kuznetsova, L.I.; Likholobov, V.A. J.Mol.Cat.A. 1996, 108, 135.

Table 1. Shift in potential of the tungsten-oxo processes in a multilayer film of $Fe(bpy)_3^{2+}$-$P_2W_{18}O_{62}^{6-}$, upon increasing pH.

pH	***$E_{1/2}$ (V) 1st W couple (vs. Ag/AgCl)***	***$E_{1/2}$ (V) 2nd W couple (vs. Ag/AgCl)***	***$E_{1/2}$ (V) 3rd W couple (vs. Ag/AgCl)***
2.0	-0.257	-0.434	-0.672
2.5	-0.289	-0.472	-0.714
3.0	-0.320	-0.503	-0.749
3.5	-0.355	-0.546	-0.795
4.0	-0.376	-0.572	-0.823
4.5	*	-0.627	-0.879

* Couple not well defined and therefore $E_{1/2}$ could not be determined accurately.

Table 2. Percentage loss in global electroactivity of the tungsten-oxo processes in a multilayer film of $Fe(bpy)^{2+}$-$P_2W_{18}O_{62}^{6-}$, as a function of pH.

pH	***Number of cycles***	$[P_2W_{18}O_{62}]^{6-/7-}$	$[P_2W_{18}O_{62}]^{7-/9-}$	$[P_2W_{18}O_{62}]^{9-/11-}$
1.1	100 200	3.9 12.9	7.6 15.9	3.4 12.1
4.0	100 200	11.5 36.2	16.0 49.8	14.5 40.4

Figure Legends

Figure 1(a) Cyclic voltammograms of a 0.5mM solution of aq. Parent HPA, $P_2W_{18}O_{62}^{6-}$, in aq. 0.5M $NaHSO_4$ at a glassy carbon electrode (A=0.0707 cm^2). Scan rate = 0.05Vs^{-1}

Figure 1(b). Cyclic voltammogram of a multilayer film of $Fe(bpy)_3^{2+}$-$P_2W_{18}O_{62}^{6-}$ in aq. 0.5M $NaHSO_4$, at a glassy carbon electrode (A = 0.0707 m^2). Scan rate = 0.2Vs^{-1}

Figure 1(c). Cyclic voltammogram of a multilayer film of $Fe(bpy)_3^{2+}$-$P_2W_{18}O_{62}^{6-}$ in aq. 0.5M $NaHSO_4$, showing the increase in current with increasing scan rate, on a glassy carbon electrode (A = 0.0707 m^2). Scan rate = 0.005^{-1} Vs^{-1} to Vs^{-1}

Figure 2(a). Cyclic voltammogram of multilayer films of $Fe(bpy)_3^{2+}$-$P_2W_{18}O_{62}^{6-}$ in aq. 0.5M $NaHSO_4$ showing the increase in current with increasing layers on a glassy carbon electrode(A = 0.0707 m^2). [Shown are 2 bilayers (inner curve) to 11 bilayers (outer curve)]. Scan rate = 0.05Vs^{-1}

Figure 2(b). Plot of number of alternating layers of $Fe(bpy)_3^{2+}$ and $P_2W_{18}O_{62}^{6-}$ versus surface coverages, on a glassy carbon electrode (A = 0.0707 m^2)

Figure 3(a). Cyclic voltammogram of a multilayer film of $Fe(bpy)_3^{2+}$-$P_2W_{18}O_{62}^{6-}$ in aq. 0.5M $NaHSO_4$, in which the outer layer is cationic, showing the increase in current of the $Fe^{2+/3+}$ redox process **when 4 (inner curve), 8, 12, 16 and 20 (outer curve) layers are present** on a glassy carbon electrode (A = 0.0707 m^2). Scan rate = 0.05Vs^{-1}

Figure 3(b). Cyclic voltammogram of a multilayer film of $Fe(bpy)_3^{2+}$-$P_2W_{18}O_{62}^{6-}$ in aq. 0.5M $NaHSO_4$, in which the outer layer is cationic, showing the decrease in current upon cycling the film for 700 cycles, on a glassy carbon electrode (A = 0.0707 m^2). (Shown, from the outer curve, are the 1^{st}, 101^{st}, 201^{st}, 301^{st}, 401^{st}, 501^{st}, 601^{st} and 701^{st} cycles). Scan rate = $0.05Vs^{-1}$

Figure 4(a). Plots of the absorbance at 244.6 nm of multilayer films of $Fe(bpy)_3^{2+}$-$P_2W_{18}O_{62}^{6-}$ on ITO/quartz slides, as a function of the number of $Fe(bpy)_3^{2+}$-$P_2W_{18}O_{62}^{6-}$ bilayers adsorbed

Figure 4(b). Plots of the absorbance at 307.2 nm of multilayer films of $Fe(bpy)_3^{2+}$-$P_2W_{18}O_{62}^{6-}$ on ITO/quartz slides, as a function of the number of $Fe(bpy)_3^{2+}$-$P_2W_{18}O_{62}^{6-}$ bilayers adsorbed

Figure 5(a). Cyclic voltammogram of 1 mM of ferricyanide in aq. 0.5M $NaHSO_4$, at a bare glassy carbon electrode (A = 0.0707 m^2). Scan rate = $0.05Vs^{-1}$

Figure 5(b). Cyclic voltammogram of multilayer film of $Fe(bpy)_3^{2+}$-$P_2W_{18}O_{62}^{6-}$ in aq. 0.5M $NaHSO_4$, at a glassy carbon electrode (A = 0.0707 m^2) . Scan rate = $0.05Vs^{-1}$

Figure 5(c). Cyclic voltammogram of multilayer of $Fe(bpy)_3^{2+}$-$P_2W_{18}O_{62}^{6-}$ + 1mM ferricyanide in aqueous 0.5M $NaHSO_4$, at a glassy carbon electrode (A = 0.0707 m^2). Scan rate = $0.05Vs^{-1}$

Figure 6(a). Cyclic voltammogram of 0.5mM $NaNO_2$ at bare glassy carbon electrode (A = 0.0707 m^2) in aqueous pH 4.0 buffer. Scan rate = 0.05Vs^{-1}

Figure 6(b). Cyclic voltammogram of a multilayer film of $Fe(bpy)_3^{2+}$- $P_2W_{18}O_{62}^{6-}$ + 0.4mM $NaNO_2$ **(lower curve)** in aqueous pH 4.0 buffer. Scan rate = 0.05Vs^{-1}.

Figure 6(c). Graph of nitrite concentration versus catalytic current for $Fe(bpy)_3^{2+}$-$P_2W_{18}O_{62}^{6-}$ multilayer film at glassy carbon electrode (A = 0.0707 m^2)

Figure 7(a). Cyclic voltammogram of 0.5mM $NaBrO_3^-$ at a bare glassy carbon electrode (A = 0.0707 m^2) in aqueous 0.5M $NaHSO_4$. Scan rate = 0.05Vs^{-1}.

Figure 7(b). Cyclic voltammogram of a multilayer film of $Fe(bpy)_3^{2+}$- $P_2W_{18}O_{62}^{6-}$ + 0.4mM $NaBrO_3^-$ **(lower curve)** in aqueous 0.5M $NaHSO_4$. Scan rate = 0.05Vs^{-1}.

Figure 7(c). Graph of bromate concentration versus catalytic current for $Fe(bpy)_3^{2+}$-$P_2W_{18}O_{62}^{6-}$ multilayer film at glassy carbon electrode (A = 0.0707 m^2)

Figure 8(a). Cyclic voltammogram of 0.5mM H_2O_2 at a bare glassy carbon electrode (A = 0.0707 m^2) in aqueous 0.5M $NaHSO_4$. Scan rate = 0.05Vs^{-1}.

Figure 8(b). Cyclic voltammogram of a multilayer film of $Fe(bpy)_3^{2+}$- $P_2W_{18}O_{62}^{6-}$ + 0.4mM H_2O_2 **(lower curve)** in aqueous 0.5M $NaHSO_4$. Scan rate = $0.05Vs^{-1}$.

Figure 8(c). Graph of hydrogen peroxide concentration versus catalytic current for $Fe(bpy)_3^{2+}$-$P_2W_{18}O_{62}^{6-}$ multilayer film at glassy carbon electrode (A = 0.0707 m^2)

Figure 1(a)

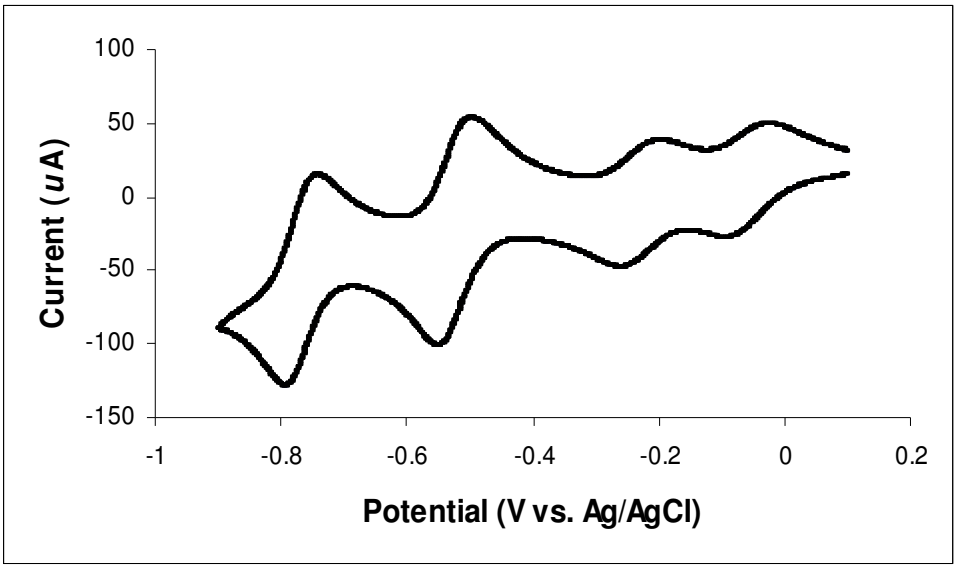
100
50
0
-50
-100
-150
Current (uA)
-1
-0.8
-0.6
-0.4
-0.2
0
0.2
Potential (V vs. Ag/AgCl)

Figure 1(b).

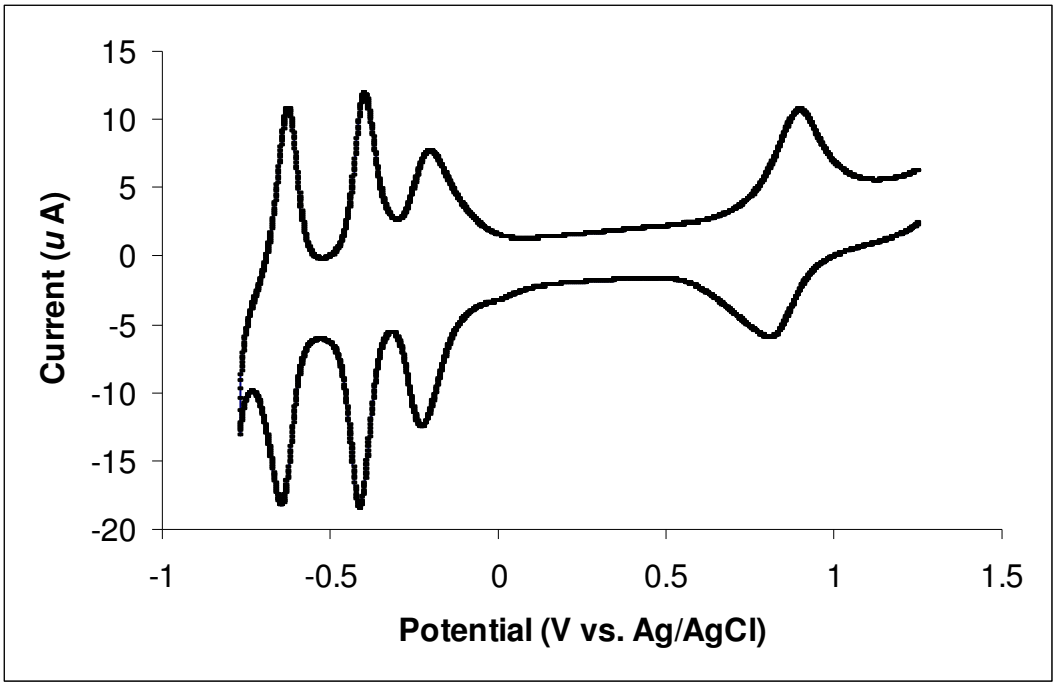

Figure 1(c).

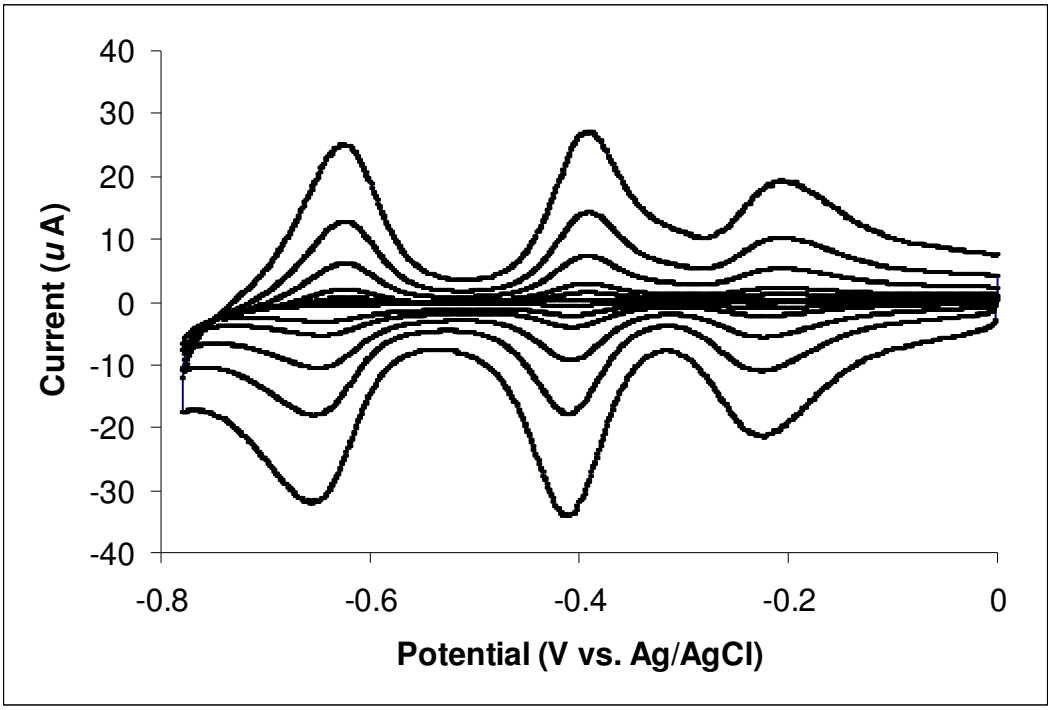
40
30
20
10
0
-10
-20
-30
-40
Current (u A)
-0.8
-0.6
-0.4
-0.2
0
Potential (V vs. Ag/AgCl)

Figure 1(d)

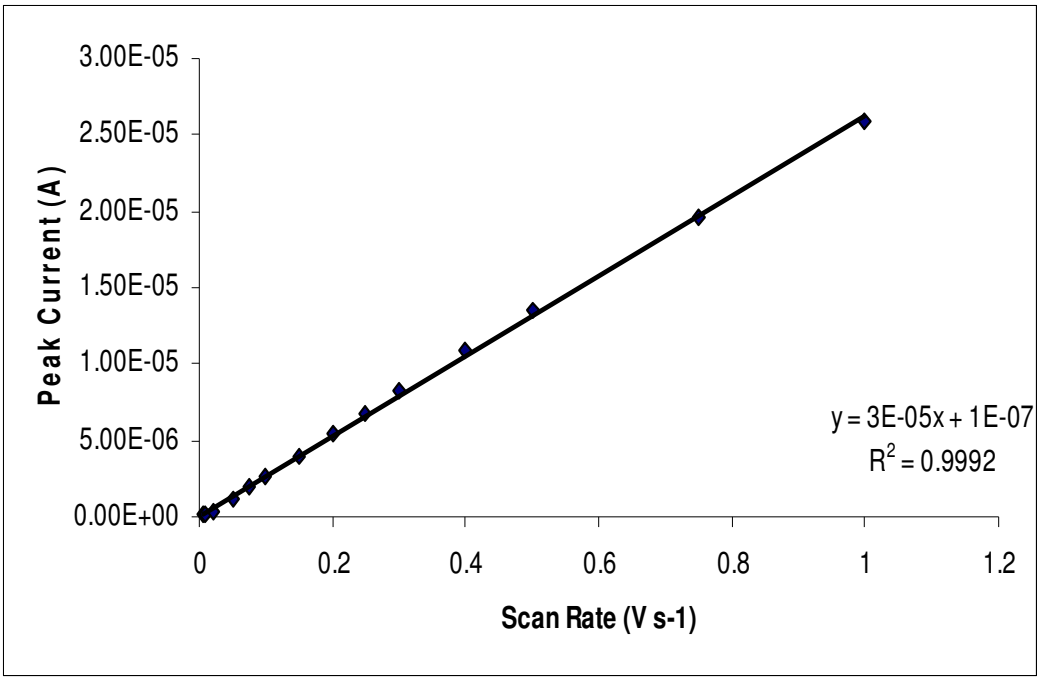
3.00E-05
2.50E-05
2.00E-05
1.50E-05
1.00E-05
5.00E-06
0.00E+00
Peak Current (A)
0
0.2
0.4
0.6
0.8
1
1.2
Scan Rate (V s-1)
y = 3E-05x + 1E-07
R2 = 0.9992

Figure 2(a).

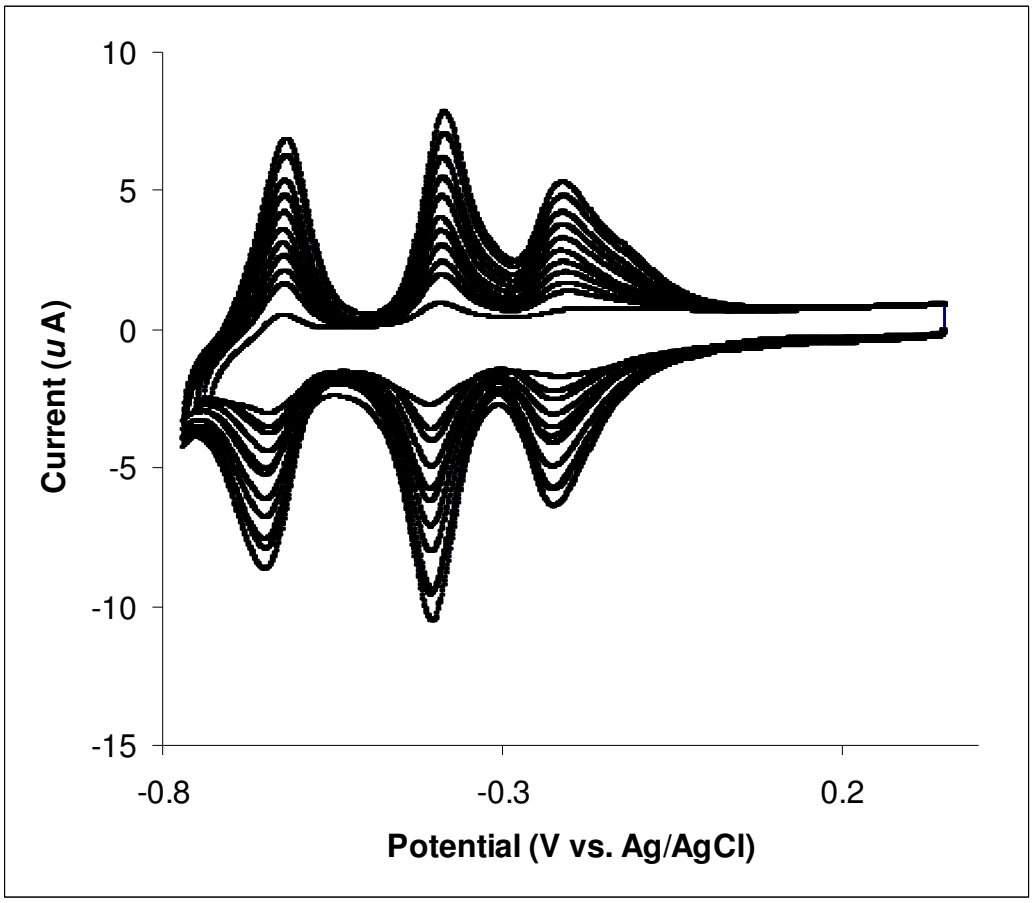

Figure 2(b).

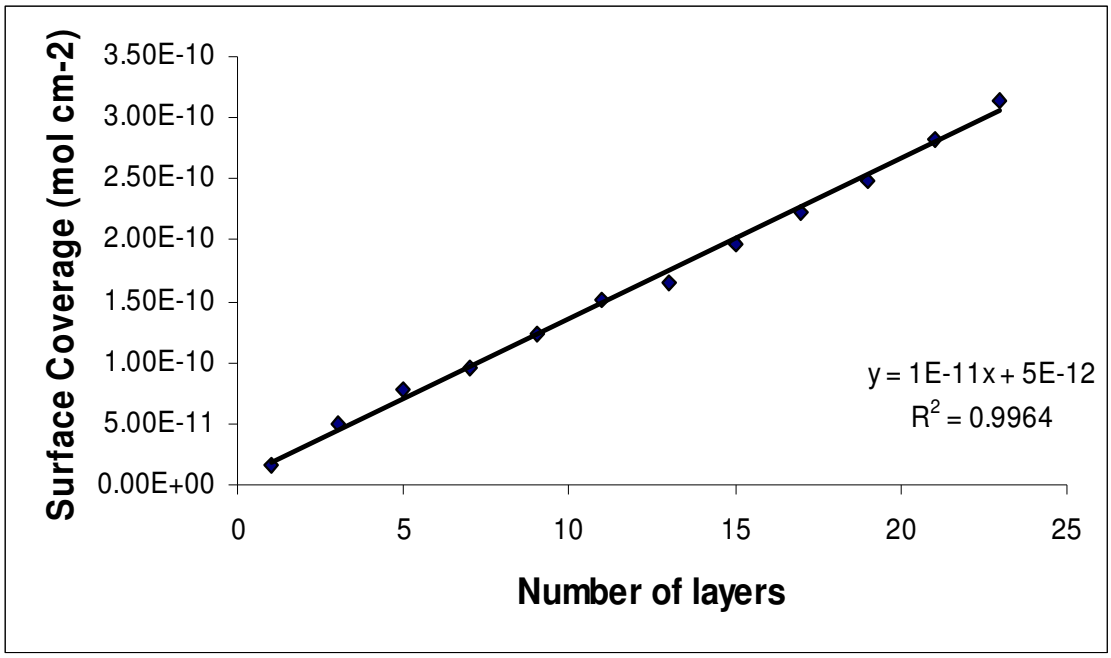
Surface Coverage (mol cm-2)
3.50E-10
3.00E-10
2.50E-10
2.00E-10
1.50E-10
1.00E-10
5.00E-11
0.00E+00
0
5
10
15
20
25
Number of layers
y = 1E-11x + 5E-12
R2 = 0.9964

Figure 3(a).

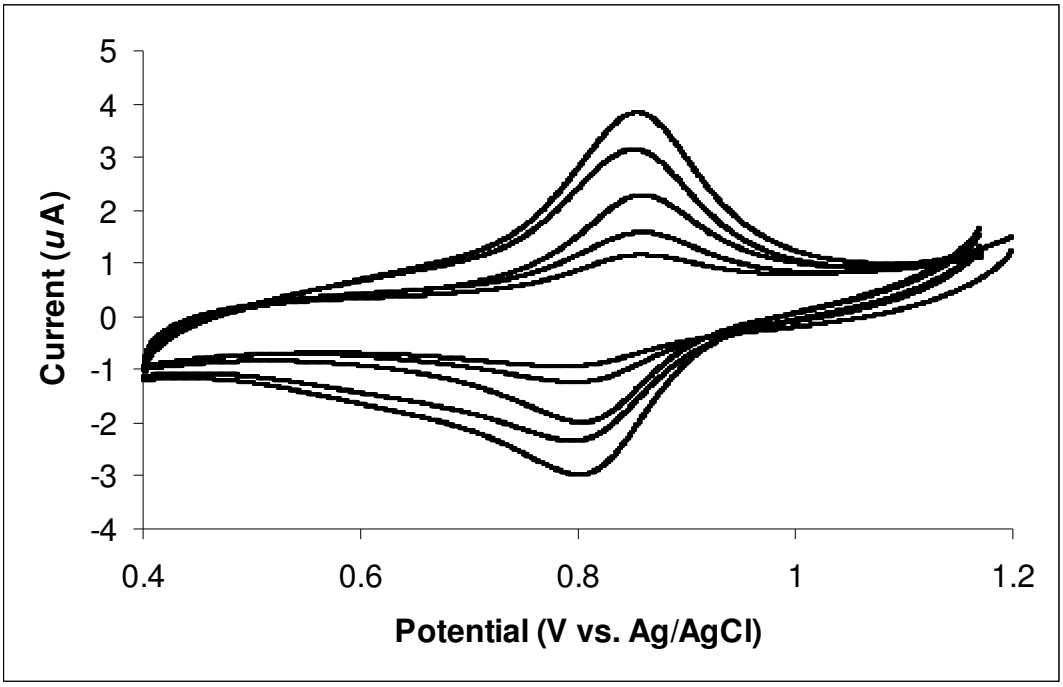

Figure 3(b).

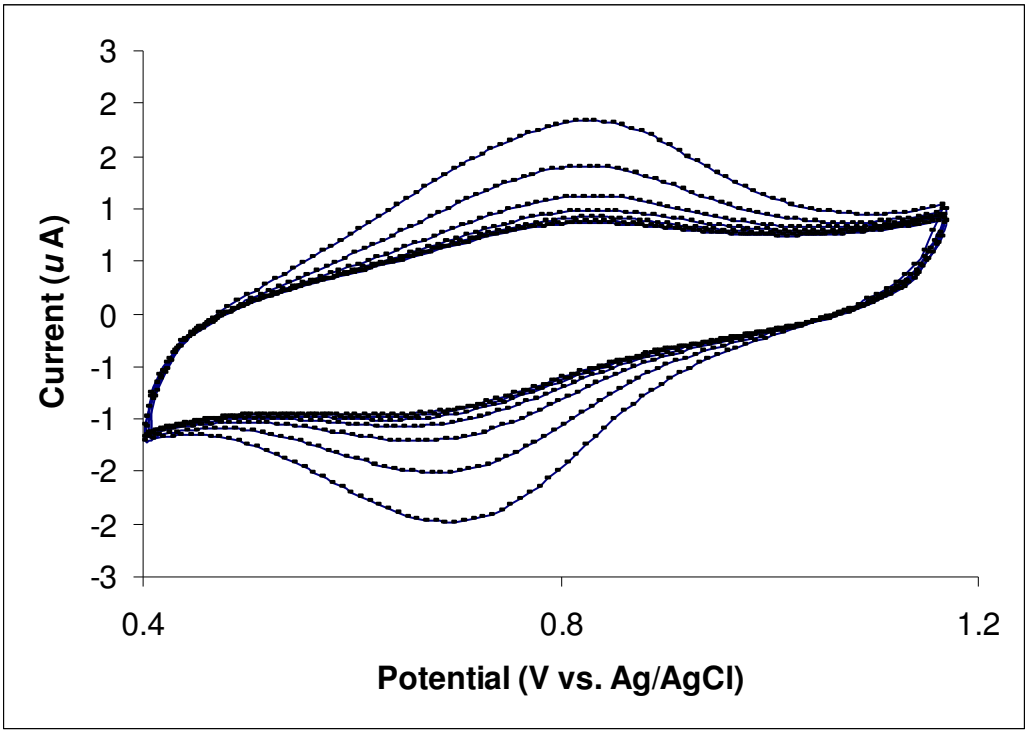

Figure 4(a).

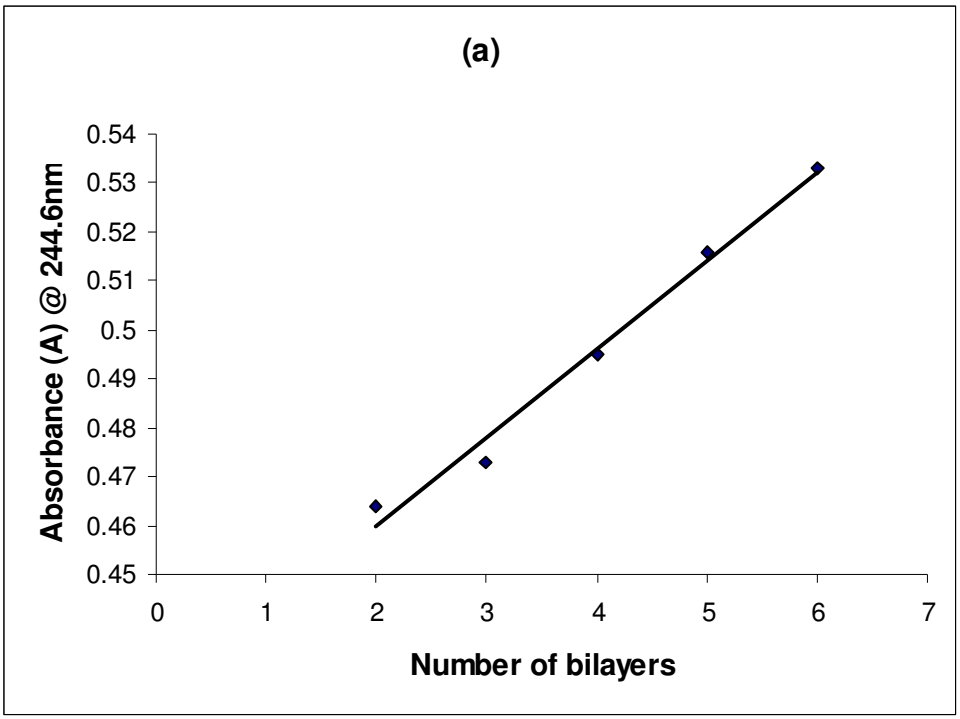
(a)
Absorbance (A) @ 244.6nm
0.54
0.53
0.52
0.51
0.5
0.49
0.48
0.47
0.46
0.45
0
1
2
3
4
5
6
7
Number of bilayers

Figure 4(b).

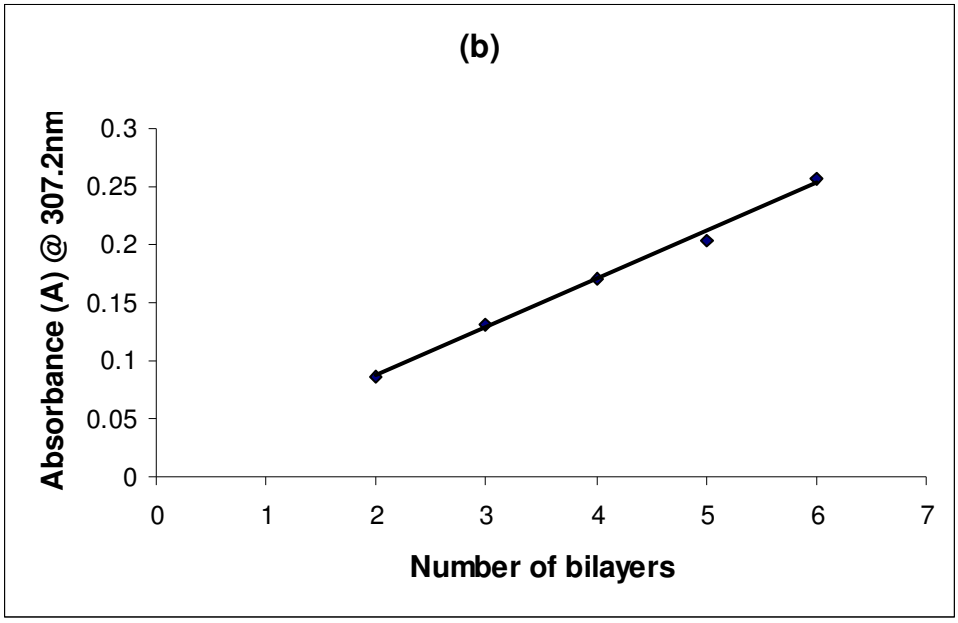
(b)
Absorbance (A) @ 307.2nm
0.3
0.25
0.2
0.15
0.1
0.05
0
0
1
2
3
4
5
6
7
Number of bilayers

Figure 5(a)

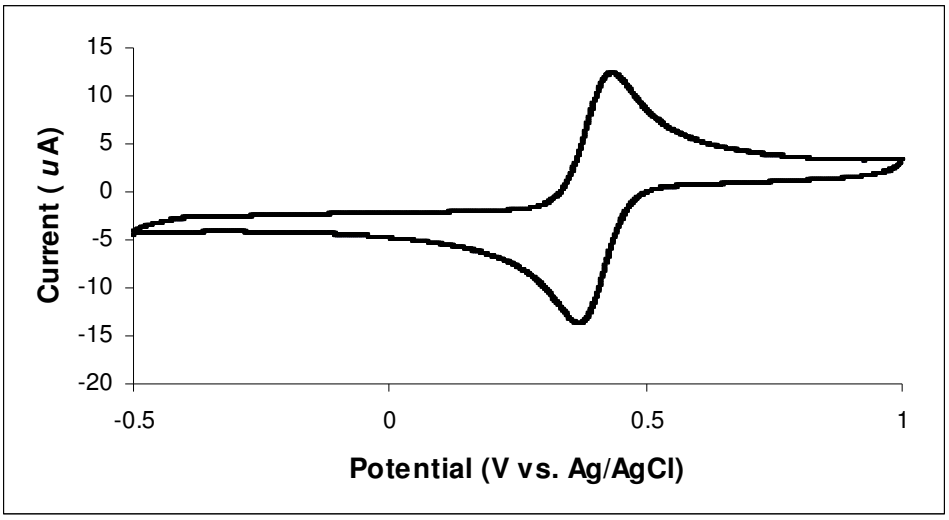

Figure 5(b)

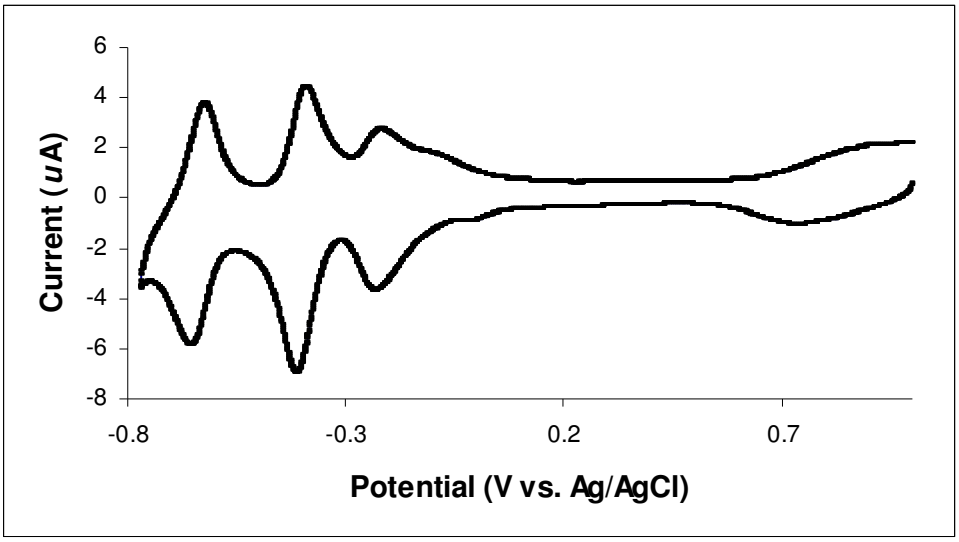

Figure 5(c)

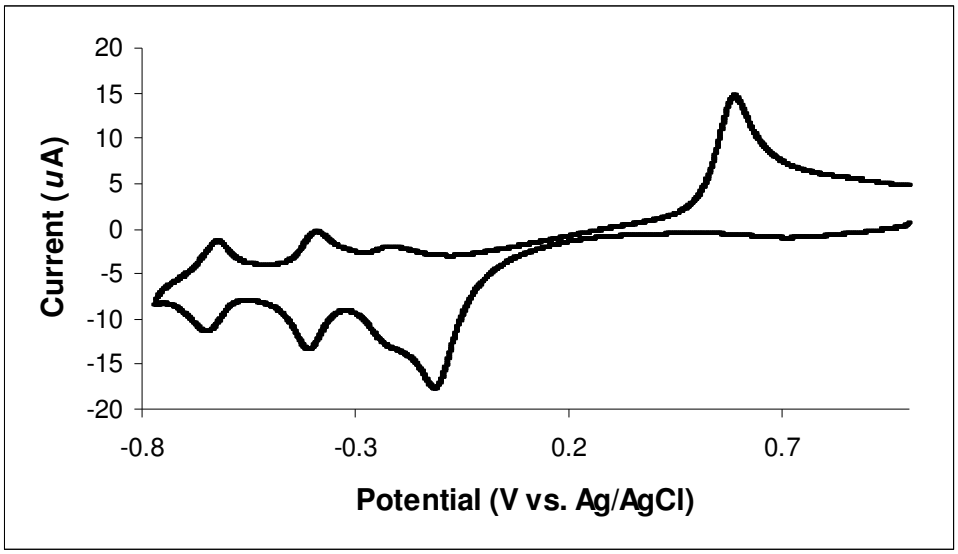
20
15
10
5
0
-5
-10
-15
-20
Current (uA)
-0.8
-0.3
0.2
0.7
Potential (V vs. Ag/AgCl)

Figure 6(a).

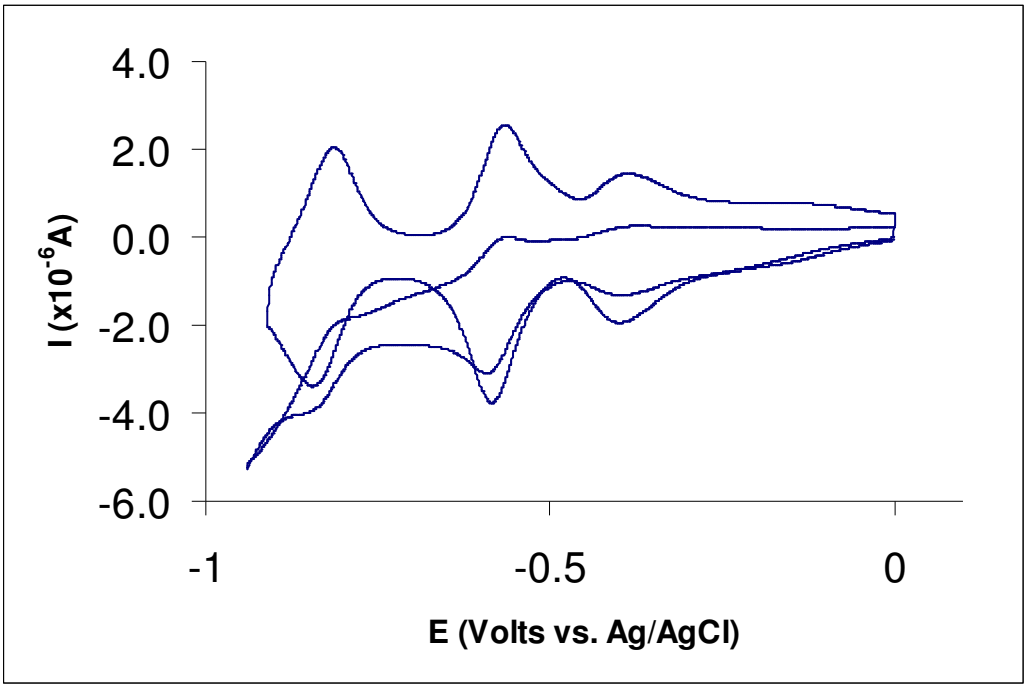

Figure 6(b)

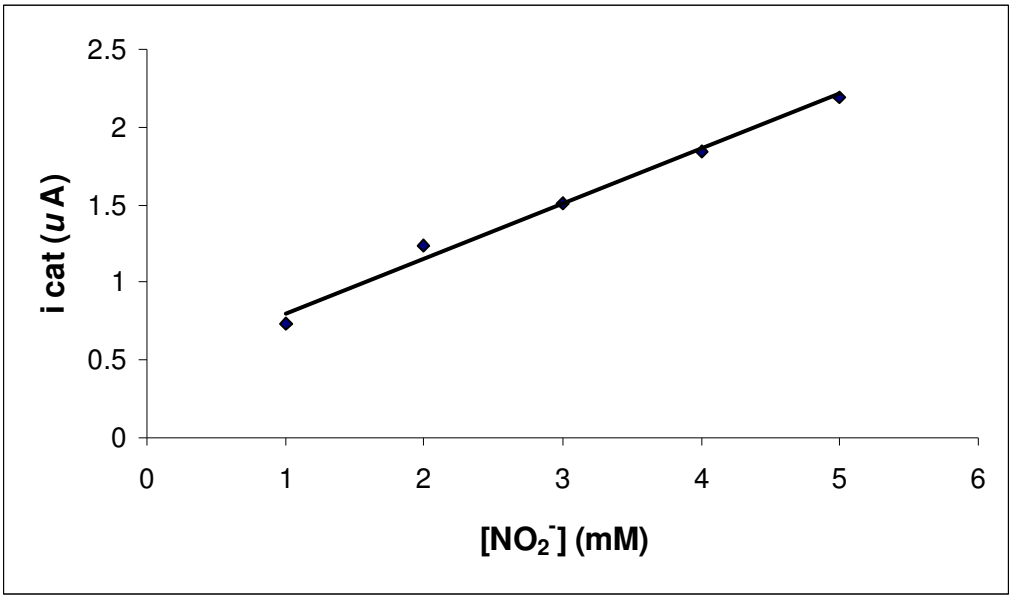

Figure 7(a).

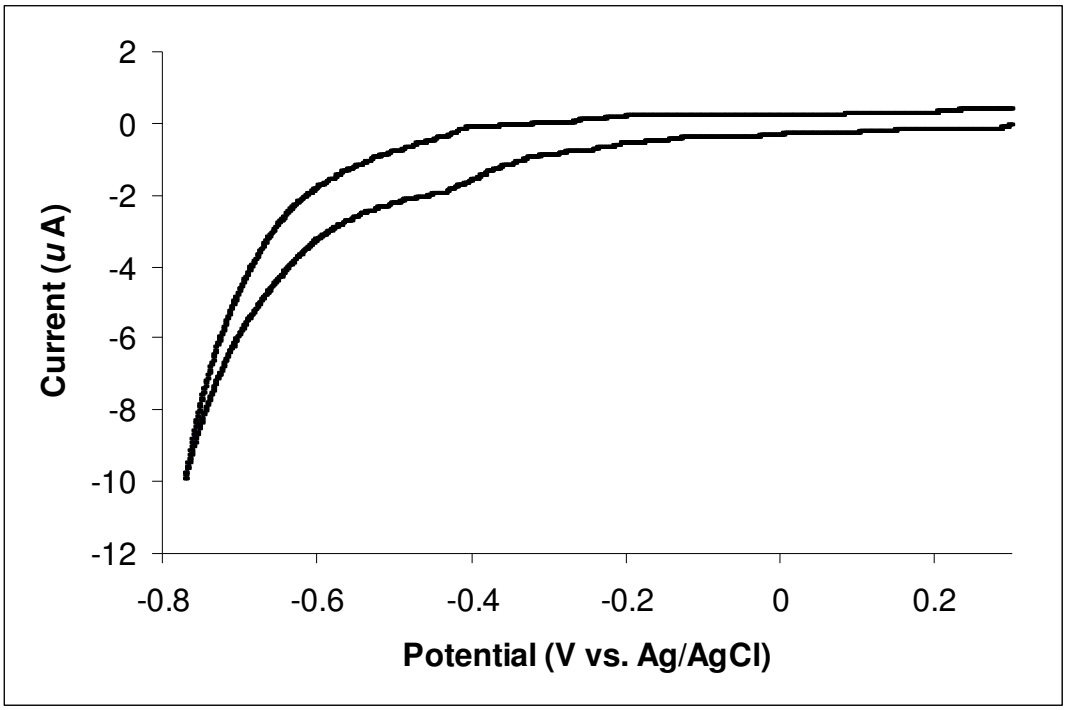

Figure 7(b).

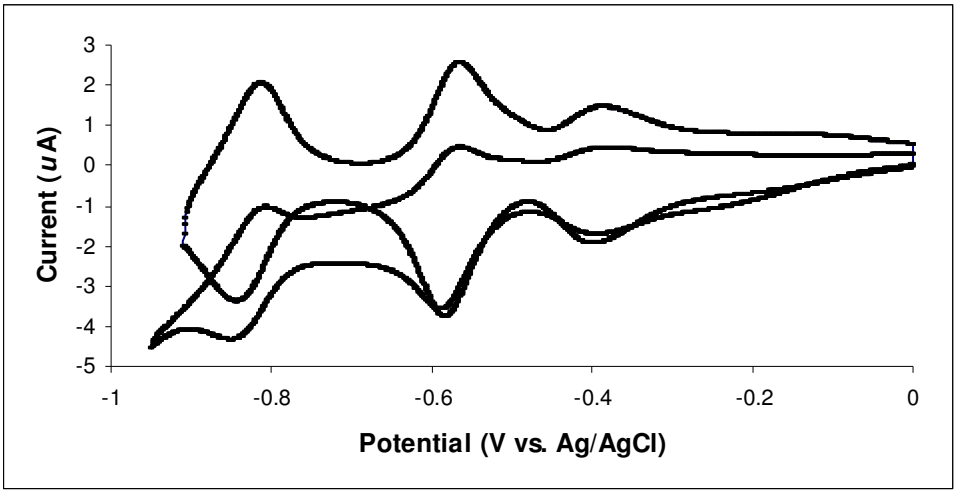

Figure 7(c).

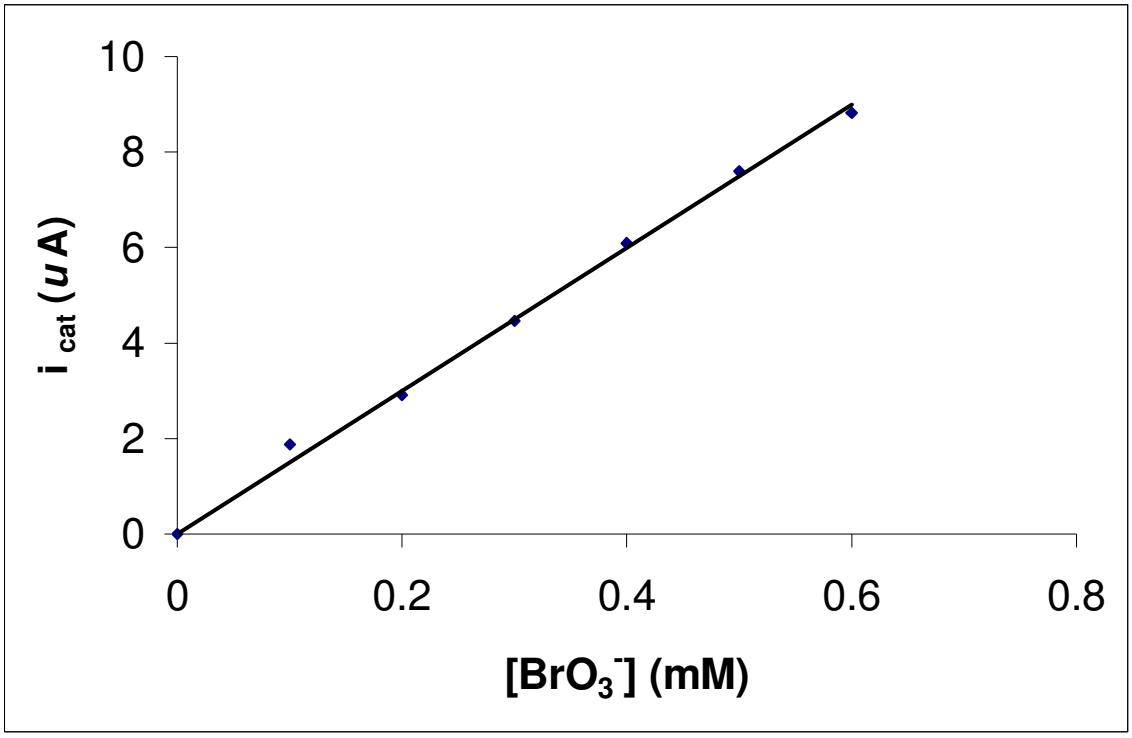

Figure 8(a)

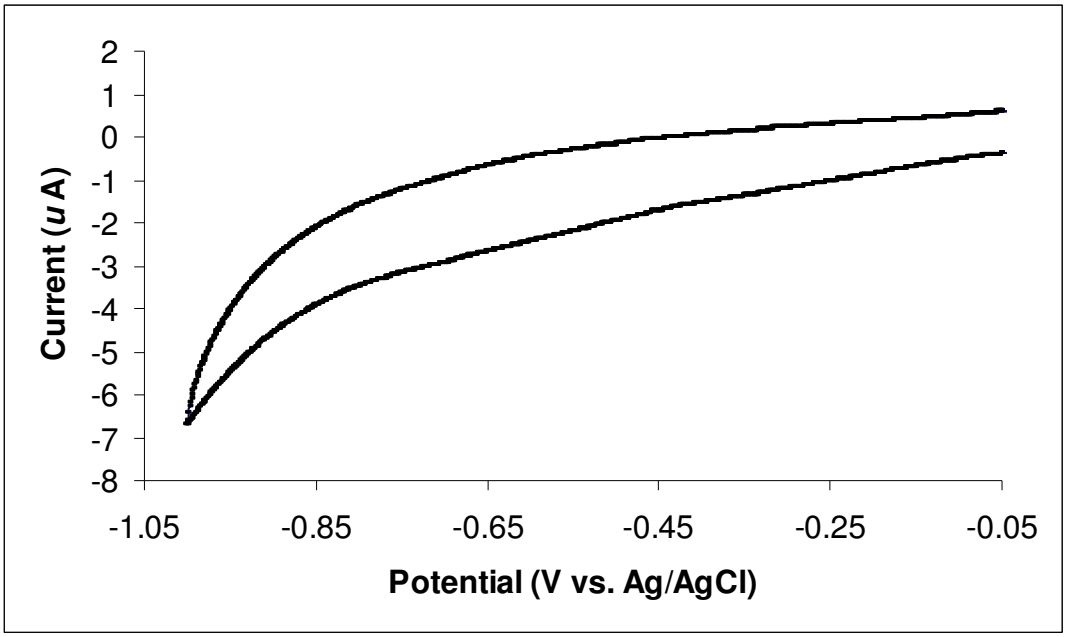
2
1
0
-1
-2
-3
-4
-5
-6
-7
-8
Current (uA)
-1.05
-0.85
-0.65
-0.45
-0.25
-0.05
Potential (V vs. Ag/AgCl)

Figure 8(b).

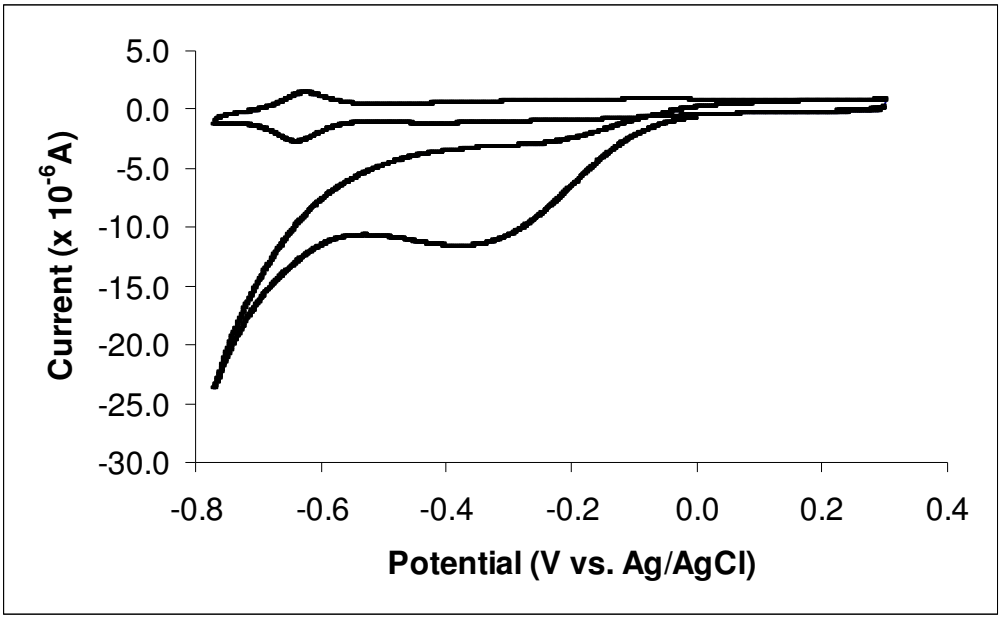
5.0
0.0
-5.0
-10.0
-15.0
-20.0
-25.0
-30.0
Current (x 10-6A)
-0.8
-0.6
-0.4
-0.2
0.0
0.2
0.4
Potential (V vs. Ag/AgCl)

Figure 8(c)